Directed Energy "Funneling" Mechanism for Heme Cooling Following Ligand Photolysis or Direct Excitation in Solvated Carbonmonoxy Myoglobin

Diane E. Sagnella and John E. Straub*

Department of Chemistry, Boston University, Boston, Massachusetts 02215

Received: February 28, 2001; In Final Form: May 14, 2001

The kinetic energy relaxation of photolyzed heme in myoglobin was investigated using molecular dynamics simulations. Following photolysis, the heme was found to lose most of its excess kinetic energy within 10 ps. The kinetic energy decay was found to be a single exponential with a time constant of 5.9 ps in agreement with the experimental observations of Lim, Jackson and Anfinrud [*J. Phys. Chem.* **100**, 12 043 (1996)]. The flow of kinetic energy was found to occur primarily through nonbonded contacts. The heme doming motion causes collisions with nearby residues and large scale collective motion in the protein. However, the strong electrostatic interaction of the isoproprionate side chains, and the solvating water appears to be the single most important "doorway" for dissipation of excess kinetic energy in the heme. Those water molecules in close contact with the heme side chains were found to "warm" in less than 1.0 ps. Direct energy transfer from the heme to the protein is found to occur by "through projectile" (ligand collisions with the distal heme pocket residue), "through bond" (heme bond to proximal histidine), and "through space" (nonbonded collisional) channels. These results provide strong evidence for a spatially directed "funneling" of kinetic energy through the heme side chains to the surrounding solvent suggested by Hochstrasser and co-workers.

1. Background and Significance

During the vibrational energy relaxation (VER) process, excess energy can flow into or out of reactive modes, thus controlling the rates of chemical reactions. It is therefore of great interest to understand the time scales and mechanisms involved in this fundamental process. For years, scientists have studied VER phenomena by monitoring the flow of energy from excited modes into the surrounding bath which may be composed of *intra*molecular vibrational modes and the *inter*molecular surroundings. The study of the flow of excess vibrational energy into or out of vibrational modes is a fundamental component of the ongoing effort to understand ultrafast conformational changes and reorganization of protein structure as a result of the binding or release of substrate molecules.[1−17]

Computer simulations have contributed to our understanding of VER processes.[9,18−23] For the case of vibrational energy relaxation in solvated diatomic molecules, it has proved possible to make a detailed analysis of the coupling between the system and the bath modes and the mechanism and time scales for vibrational relaxation. However, the effort to extend such detailed analyses to more complex systems has been hindered by the fact that there is often no clean separation into system and bath modes.[24]

Since the pioneering work of Hochstrasser and co-workers,[25] it has been recognized that a detailed analysis of vibrational relaxation of heme proteins can provide vital information concerning the cooperative nature of protein dynamics. Typical optical experiments have focused on the relaxation of a photodissociated ligand, in particular carbon monoxide. Metal carbonyls are among the most thoroughly studied[26−28] due to their exceptional electronic transitions (having high oscillator strength, large absorption coefficient, or strong electronic resonance) in the visible and ultraviolet regimes. However, there has also been a significant effort to define the time scales and pathways for vibrational energy relaxation in larger related heme protein systems including myoglobin, hemoglobin, and cytochrome *c*.

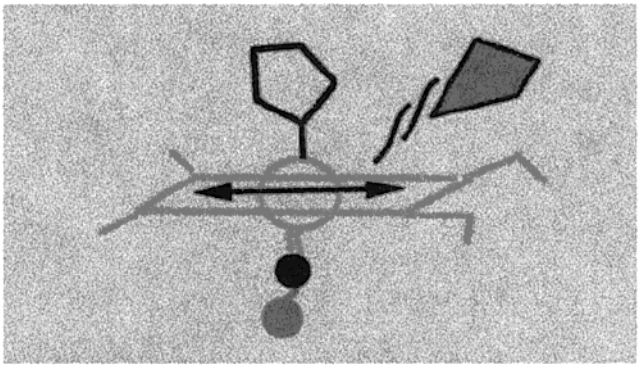

Figure 1. Depiction of the mode of excitation of an in-plane heme vibration.

The heme chromophore in myoglobin has only one direct link with the protein − a bond between the iron atom and a nitrogen atom of the proximal histidine, His93. In the ligated state, the iron is six coordinate and the Fe−N bond is orthogonal to the heme plane and, consequently, to the heme's in-plane vibrational modes. This orientation decouples the Fe−N stretch from the heme's in-plane vibrations, making through bond transfer from in-plane heme vibrations an unlikely doorway for excess vibrational energy relaxation (Figure 1).

Following photolysis, the heme becomes five coordinate and assumes a domed geometry inducing tertiary and quaternary structural changes in the protein (see Figure 2). As such, through bond transfer of excess kinetic energy from the heme to the protein is more likely following ligand photolysis than following direct excitation of in-plane heme vibrations. Frauenfelder and

* To whom correspondence should be addressed. Tel: (617)353-6816. E-mail: straub@bu.edu.

10.1021/jp0107917 CCC: $20.00
Published on Web 06/28/2001

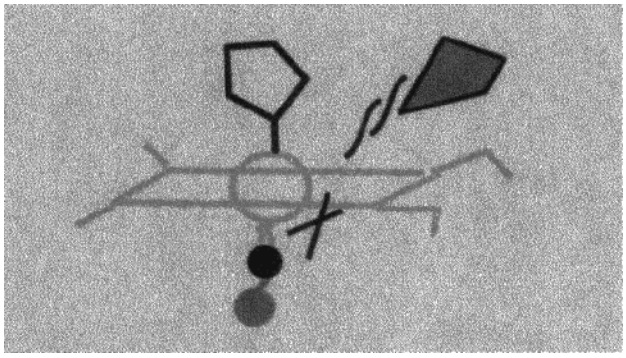

Figure 2. Depiction of the mode of excitation of the heme through the photolysis of the carbon monoxide ligand.

co-workers have described the process by which myoglobin returns to equilibrium as a "protein quake."[29] In hemoglobin, these changes are coupled between subunits making hemoglobin a prime example of molecular cooperativity and allostery.

Summarized below are a variety of probes of the relaxation following ligand photolysis, or following direct excitation of the heme, that have provided detailed information on the time scales of heme relaxation and the transfer of energy between the protein and surrounding solvent. A fine review of this subject has recently been presented by Mizutani and Kitagawa.[30]

1.1. Simulations of Heme Cooling in Myoglobin. Computer simulations of relaxation in heme proteins began with the pioneering study of myoglobin and cytochrome *c* by Henry, Eaton, and Hochstrasser.[9,23,31] By adding 54 or 81 kcal/mol of kinetic energy to the chromophore, they simulated the process of heme absorption of a 530 or 353 nm pulse, respectively. The vibrational dynamics was found to be strongly influenced by the density of the intramolecular vibrational modes, which are responsible for intramolecular vibrational energy redistribution (IVR). As a result, the excess kinetic energy was found to be almost instantaneously redistributed among the heme's vibrational modes.

The authors found that the heme had effectively cooled within 20−40 ps. In fact, approximately 50% of the excess energy was found to relax within the first 4.0 ps. The study was done in vacuo and the authors proposed that the explicit inclusion of solvent may increase the rate of the vibrational relaxation process.

1.2. Experimental Probes of Heme Cooling. By exciting the heme with a 500 nm pulse, time domain experiments have been used to monitor the decay of the vibrationally excited modes, as well as the buildup of energy in the accepting modes.[32,33] Time-resolved Raman studies[32,33] have found that the excess energy within the heme is transferred to modes of the protein in approximately 5 ps. After photoexciting the heme in deoxyhemoglobin with a 532 nm pulse, Lingle and co-workers found that the heme's excess vibrational energy was completely dissipated within 15 ps.[33] On the basis of a careful analysis of Raman scattering for a number of metalloproteins, Li, Sage, and Champion identified a time constant of 4 ps for heme cooling.[34] In a study of heme cooling following photoexcitation of the heme in myoglobin, Lim, Jackson and Anfinrud reported a single-exponential time constant of 6.2 ± 0.5 ps for cooling of the electonically relaxed heme.[35]

Kitagawa and co-workers[16] probed the relaxation of the ν_4 in-plane vibrational mode of the heme in myoglobin using Resonance Raman spectroscopy (see Figure 1). Monitoring the time behavior of the relaxation process, they concluded that thermal energy relaxation of the heme exhibited a biphasic decay with time constants of 3.0±1.0 ps and 25.0±14.0 ps. Approximately 93% of the energy was found to relax on the shorter time scale.

1.3. Experimental Measures of Protein−Solvent Energy Transfer. Miller and co-workers have employed transient phase grating spectroscopy[13] to monitor the change in the index of refraction of the solvent due to photoinduced changes in the system's mass density that accompany thermal expansion. They demonstrated that heme relaxation and energy transfer to the surrounding solvent occurs on a time scale of less than 20 ps.[13,36]

A detailed analysis of the time scales and pathways for energy flow between the protein and the solvent was presented by Hochstrasser and co-workers.[37] Following the excitation of the protein using a 580 nm pulse, the infrared transmission of the D_2O solvent was monitored on the picosecond time scale. A shift was observed in the roughly 1800 cm^{-1} stretching mode of D_2O and attributed to the rise in temperature following energy transfer from the protein to the solvent. The shift was found to occur in 4 ± 3 ps. By assuming that the solvent absorbance was linear in the temperature, it was determined that 60% of the energy was transferred on a time scale of 7.5 ± 2.0 ps, whereas 40% of the energy relaxed more slowly (in approximately 20 ps).

The longer time scale energy relaxation was attributed to a diffusional transfer of energy from the heme to the surrounding protein and subsequently to the solvent. The fast component was said to be a nondiffusional energy transfer through "collective motions" of the protein. The authors noted that the excitation of the heme was not expected to lead to global "tertiary" motions of the protein. However, it was suggested that the excitation may stimulate lower frequency "collective motions" of the protein.

Although the heme is, for the most part, buried in a hydrophobic pocket within the protein matrix of myoglobin, it remains in contact with surrounding solvent molecules. The protruding charged isoproprionate side chains of the heme are well solvated. It is conceivable that this could present a path by which excess energy could be released.[24] Hochstrasser and co-workers considered direct energy transfer through the heme side chains to the solvent: "Is it possible that the vibrational energy of the heme could be transferred directly to the surrounding water by the solvent-induced damping of these stimulated side chain motions?" They noted that "there is no precedent for such highly directed energy funneling in molecular relaxation processes."[37]

In this paper, we present our computational study of the heme relaxation process in myoglobin. We simulate and analyze the details of heme relaxation following ligand photolysis. We find strong evidence for the mechanism of "highly directed energy funneling" suggested by Hochstrasser and co-workers. The time scale for the energy transfer to the solvent is in good agreement with the fast component seen in experimental studies of heme relaxation and water excitation. Our simulations suggest that the relaxation process is best fit by a single-exponential function of time. There is no evidence of substantial long time scale relaxation on the order of 20−40 ps in the solvated protein.

2. Computational Models and Methods

The sperm whale myoglobin molecule[38] was placed in a 56.70 × 56.70 × 37.712 $Å^3$ box and simulated using periodic boundary conditions. A previously equilibrated box of TIP3P water molecules[39] was layed over the protein and any water molecule whose oxygen atom was within 2.5 Å of a non-hydrogen protein atom was removed. The all hydrogen protein

(version 22) parameter set[40] of the CHARMM[41] simulation program was used. The system, in its entirety, was composed of 11 499 atoms; 2551 myoglobin atoms, 2982 water molecules and the two atoms of the singl CO molecule. Steepest descent energy minimization was used to relieve bad contacts and relax unusual strain.

2.1. Molecular Dynamics Simulation. The molecular dynamics was simulated using the Verlet algorithm with a time step of 1.0 fs. The nonbonded potential was truncated using a group switching function extending from 9.5 to 11.5 Å. The temperature was increased slowly to 300 K using the following protocol. From 0 to 150 K, the temperature was increased 10% after every two picoseconds of molecular dynamics by randomly sampling the atomic velocities from a Maxwell distribution. The criteria for velocity resampling was based on a 5% temperature window. From 150 to 215 K, the temperature was scaled by 5% every two picoseconds and the window became 2.5% of the current temperature. When the temperature reached 215 K, the temperature window became constant at an absolute value of 5 K with an interval of 4 ps between velocity resamplings.

Once a temperature of 300 K was reached, 20 ps of constant temperature molecular dynamics was run in which the temperature was checked every 10 fs. During the last 10 ps, the average temperature remained within the 5 K window and there was no need to resample the atomic velocities. At this point, it was assumed that an equilibrium state had been reached. The system was allowed to evolve for an additional 50 ps. Coordinates and momenta were saved every 5 ps for a total of 10 configurations. Each of those configurations was then run for 15 ps, while resampling the velocities every 3 ps. The system was then allowed to relax for 2 ps before the trajectories were collected.

Ten 30 ps microcanonical trajectories were generated for both the nonequilibrium (photolyzed) and the equilibrium (nonphotolyzed) states. The initial configuration for each photolyzed trajectory was identical to the corresponding nonphotolyzed trajectory at the moment of photolysis with the exception of the velocities of the 73 heme atoms.

2.2. Preparation of the Photolyzed State. During a typical optical photolysis experiment, 10 000−20 000 cm^{-1} of excess energy is deposited into the heme. To approximate the photolysis event, approximately 88 kcal/mol of excess kinetic energy, equivalent to two 500 nm photons, was deposited in the heme. The excess kinetic energy was distributed according to a Maxwell distribution of velocities. With the excess kinetic energy equipartitioned over the 213 vibrational modes of the heme, the temperature of the heme increased by 400 K.

In the photolyzed state, the three site model of carbon monoxide, developed by Straub and Karplus,[7,11] was employed. In that model, to reproduce the dipole and quadrupole moments of the free CO ligand, charges are placed on the carbon and oxygen atoms as well as the molecule's center of mass. The remaining potential parameters were those of the standard (version 22) CHARMM force field.[40]

2.3. A Measure of the Rate of Local Kinetic Energy Relaxation. The ergodic measure provides a means of determining the time scale for the self-averaging of a given property in a many body system.[42] The fluctuation metric is defined

$$\Omega(t) = \sum_{j}^{N} [f_j(t) - \bar{f}(t)]^2 \qquad (1)$$

where $f_j(t)$ is the time average for atom j of property $F(t)$ of the system and $\bar{f}(t)$ is the average over all N atoms of property $F(t)$ at time t. Here, we take $F_j(t)$ to be the kinetic energy of the jth atom. If the system is self-averaging, the function $\Omega_{KE}(t)$ in eq 1 decays to zero as

$$\Omega_{KE}(t)/\Omega_{KE}(0) \sim \frac{1}{D_{KE}t} \rightarrow 0 \qquad (2)$$

The slope of $\Omega_{KE}(t)$ is proportional to the generalized diffusion constant D_{KE} for the observable − the kinetic energy. Thirumalai and Mountain[42] have related the mean square fluctuations in the total energy metric to the generalized diffusion constant describing the rate of exploration of the energy space. The argument may be extended in a straightforward way to the case of the kinetic energy.[24] If we assume that the microscopic motion is well described by a Langevin dynamics, it is possible to relate the rate of self-averaging of the atomic kinetic energy, as measured by the ergodic measure, to the static friction of a Langevin model.[24] For the kinetic energy metric and the Langevin equation, we can determine the generalized associated diffusion constant of

$$D_{KE} = \gamma_0 \qquad (3)$$

where γ_0 is the static friction. It follows that at long times

$$\text{slope}\left[\frac{\Omega_{KE}(0)}{\Omega_{KE}(t)}\right] = \gamma_0 \qquad (4)$$

Through a determination of the generalized diffusion constant for the kinetic energy metric, the friction acting on the motion of a particle in the heme, protein, or solvent may be determined with great precision.[24]

3. Results and Analysis

Simulated dynamical trajectories were used to determine the dominant time scales and pathways of kinetic energy relaxation following ligand photolysis in solvated carboxy myoglobin.

3.1. Relaxation in Photolyzed Myoglobin. The average amount of kinetic energy apportioned over the 73 atoms of the heme in the photolysis process is approximately 88 kcal/mol. The subsequent increase in temperature of the rapidly equipartitioning modes of the heme is over 400 K. The average time dependence of the nonequilibrium relaxation of the excess kinetic energy within the heme computed over our simulated trajectories is shown in Figure 3. The data are well modeled by a single exponential with a decay rate of 0.17 ps^{-1} or relaxation time of 5.9 ps. The initial decay of the kinetic energy is quite rapid; within 20 fs the kinetic energy has dropped 12.0 kcal/mol. As the heme continues to relax, the remainder of its excess kinetic energy is found to dissipate within 10 ps.

Not shown is the heme vibrational potential energy. In the preparation of the photolyzed state, the heme is also placed in a state of higher potential energy. This is due to changes in the intra- and intermolecular potentials of the heme. For the six coordinate heme iron, the heme is essentially planar. The equilibrium structure of the five coordinate heme is domed. As a result, the equilibrium bonds and angles are quite different in the photolyzed and nonphotolyzed states. In addition, in the photolyzed state the heme interacts with the CO molecule through nonbonded interactions and feels a strong repulsion due to the close proximity of the CO molecule (∼1.9 Å). At the instant of photolysis, the potential energy of the heme is increased by approximately 58.0 kcal/mol. On average, 37 kcal/mol is due to the intramolecular strain and 21 kcal/mol is due to the largely repulsive interaction with the CO molecule. The distortion is centered on the iron atom and the nitrogens directly

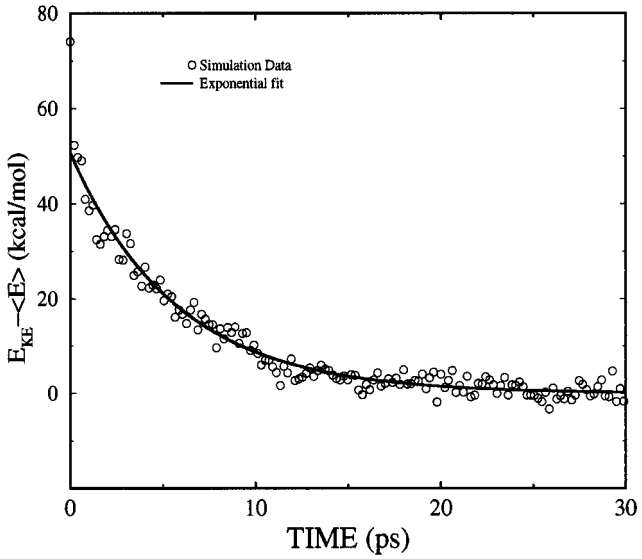

Figure 3. Exponential decay of the excess kinetic energy placed within the heme is depicted. The simulation data are represented by circles, whereas the best exponential fit is represented by the solid line. The time behavior of the kinetic energy can be adequately modeled by a single exponential with a time constant of ~5.9 ps. $\langle E\rangle$ equals the average equilibrium kinetic energy for the heme at 300 K, computed as $3Nk_BT/2$ where N is the number of atoms in the heme.

TABLE 1: Average Kinetic Energy over the Entire 30 ps and Last 15 ps of the Simulations. Preparation of the Photolyzed and Non-photolyzed States Is Described in the Text

	non-photolyzed		photolyzed	
	30 ps	15 ps	30 ps	15 ps
HEME	0.916	0.903	1.021	0.908
PROTEIN	0.899	0.899	0.908	0.907
SOLVENT			0.900	0.901

bonded to it. However, within a few femtoseconds, the energy has been redistributed evenly among the modes of the heme (see Table 1).

The observed rapid energy redistribution within the heme is consistent with the large value of the computed friction coefficients for the atoms of the heme. The great connectivity and high density of vibrational states within the heme leads to a rapid redistribution of the kinetic energy.

3.2. Kinetic Energy Dissipation. An average of 88 kcal/mol kinetic energy was added to the heme over the 10 trajectories, heating the heme by roughly 400 K. If this excess energy were redistributed equally among all the atoms of the protein and heme system, the rise in temperature would be 2.6 K. Comparing the data for energy relaxation in the nonphotolyzed and photolyzed states, we observe an increase in kinetic energy of 9 cal/mol. This translates to a rise in temperature of roughly 3.0 K. The results are summarized in Table 1.

The average kinetic energy was calculated for the heme, protein, and solvent from the 30 ps of dynamics following each simulated photolysis event. The kinetic energy is transferred rapidly from the thermally excited heme to the surrounding protein and solvent. The energy relaxation of the heme occurs well within the 20 ps window suggested by Miller.[13] In fact, a majority of the excess kinetic energy is dissipated within 5 ps of excitation.

The average kinetic energy relaxation during the *last* 15 ps of the dynamics was also examined. The kinetic energy of the nonphotolyzed heme calculated over 30 ps is 0.92 kcal/mol, whereas the average kinetic energy of the photolyzed heme is the somewhat larger 1.02 kcal/mol. The average kinetic energy over the last 15 ps of the 30 ps trajectory was found to be essentially identical for the nonphotolyzed (0.903 ± 0.020 kcal/mol) and photolyzed (0.908 ± 0.020 kcal/mol) trajectories, respectively.

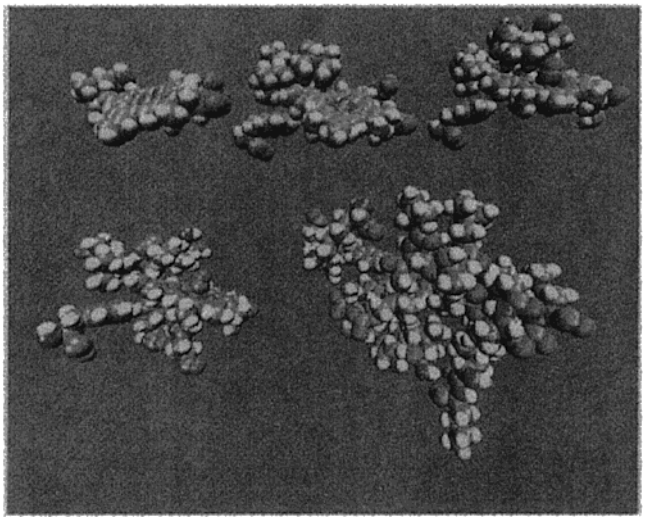

Figure 4. Redistribution of the excess kinetic energy from the heme to the surrounding protein for a representative trajectory. The redistribution of the kinetic energy follows pathways with a high degree of spatial anisotropy or directed energy "funneling."

If we examine the kinetic energy of the protein and solvent, we see that the difference in the average kinetic energy calculated at 30 ps and during the final 15 ps is minimal. This supports the observation that the excess kinetic energy is transferred on a short time scale directly to the bath. If the transfer of excess energy from the heme to its surroundings occurred on a longer time scale than that simulated, then we would expect to see a much slower rise in the temperature but one that continued to progress with time. Instead, the change in kinetic energy occurs relatively quickly and appears to be nearly complete within a few ps.

3.3. Pathways for the Kinetic Energy Relaxation. The spatial dependence of the pathway of kinetic energy relaxation was visualized in two ways. First, the angular distribution of the excess kinetic energy of all atoms, including solvent, was plotted in spherical polar coordinates. Second, instantaneous "snapshots" in the process of nonequilibrium relaxation were analyzed by tagging those atoms of the heme and protein (ignoring solvent) with a significant amount of excess kinetic energy and plotting only that subset of atoms in a space filling CPK model. The analysis below is representative of the common features of relaxation time scale and pathway observed in all of the computed trajectories.

Projected Angular Dependence of Energy "Funneling" Aniostropy. The coordinates in the dynamics trajectories were translated and rotated so that the iron atom was located at the origin and the nitrogen atoms of the heme's pyrrole rings A and B were arranged along the x- and y-axis, respectively. This transformation placed the iron atom and the four pyrrole nitrogens of the heme ring more or less in the $x-y$ plane. Figure 5 illustrates the orientation of the heme with respect to the angles θ and ϕ. θ is the angle between the z-axis and this plane; ϕ is the angle measuring rotation of the heme plane about the z-axis. Using this orientation, the four pyrrole ring nitrogens were located near $\theta = 90°$ and ϕ values of 0°, 90°, 180°, and 270° for rings A, B, C, and D, respectively.

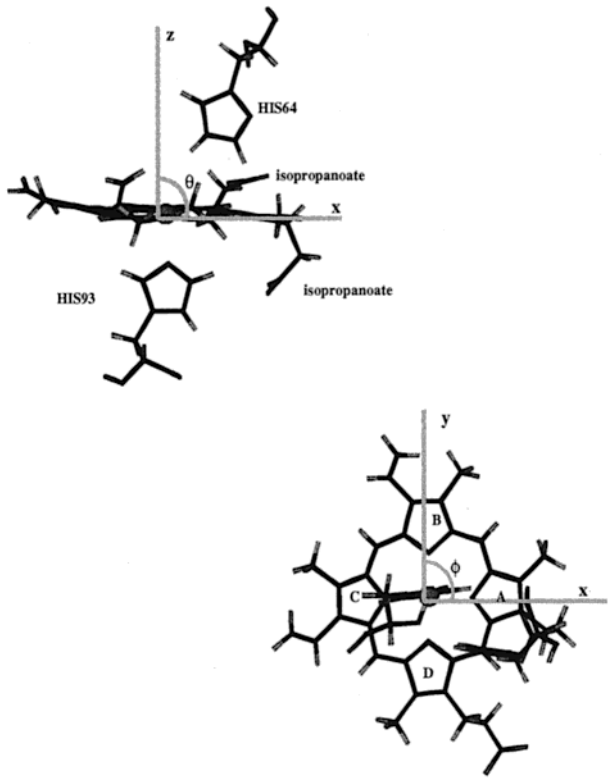

Figure 5. The heme is shown with its Fe atom at the origin and nitrogen atoms of pyrrole heme rings A and B located along the *x*- and *y*-axes, respectively. The iron atom and the four pyrrole nitrogens are roughly in the $x-y$ plane. θ is the angle the *z*-axis makes with this plane; ϕ is the angle of rotation of the heme plane.

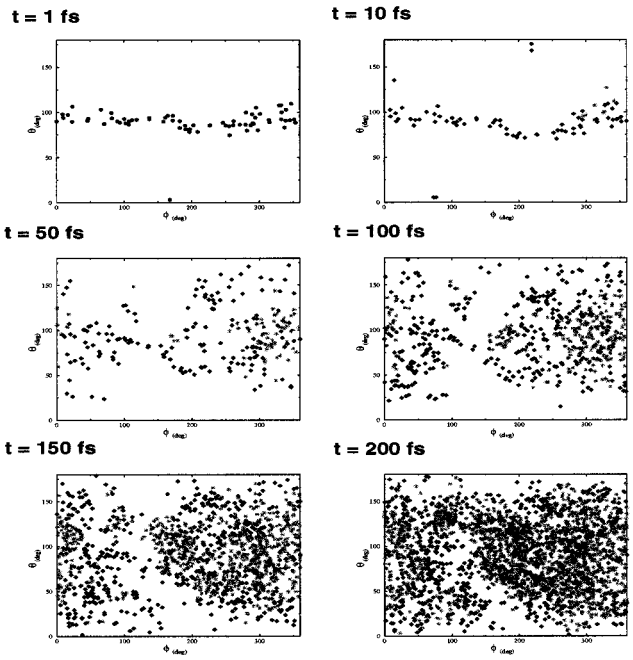

Figure 6. Redistribution of the excess kinetic energy in the heme-centered reference frame. In the initial frame, the dots show the excess kinetic energy of the heme atoms. In subsequent plots, diamonds appear for the protein and heme atoms (crosses for water molecules) with kinetic energy significantly higher than the mean value at the equilibrium temperature. The strong spatial anisotropy clearly demonstrates the directed "funneling" of excess kinetic energy through the heme side chains and into the surrounding solvent.

In Figure 6 , there are snapshots at six different observation times showing the positions (in θ and ϕ) of atoms having an excess kinetic energy that is *significantly higher* than the equilibrium average value. Both protein atoms (diamonds) and water molecules (stars) are shown. There is a strong concentration of kinetic energy, a hot spot, in the region of $\theta = 90°$ $\phi = 330°$, which is the location of the heme side chains. This plot clearly shows the "funneling" of kinetic energy from the heme through its side chains into the surrounding solvent. These calculations provide strong evidence for the strongly directed molecular energy transfer in the relaxation of the heme proposed by Hochstrasser and co-workers.[37]

Visualization of Nonequilibrium Energy Relaxation. In Figure 4 is shown snapshots of the energy redistribution in the heme and protein. Five sets of coordinates are shown from times 200, 400, 600, 800, and 1000 fs. The residues that appear contain atoms whose instantaneous excess kinetic energy exceeded a threshold of 10% of the equilibrium average. In the first snapshot, the excess kinetic energy is localized in the heme. The heme's side chains are clearly visible. Note that the proximal region lies below the plane (as plotted). For the most part, the solvent is just to the right of the heme and the protein is found above, below, and to the left.

The spreading of the kinetic energy from the heme to the protein occurs through three channels: (1) "through space" energy transfer mediated by collisions of hot heme atoms with surrounding protein atoms, (2) "through bond" energy transfer mediated by the intramolecular vibrational relaxation through the covalent bonding of the heme iron to the proximal histidine, and (3) "through projectile" energy transfer mediated by collisions with the initially supersonic CO ligand molecule as it dissociates from the heme and collides with atoms of residues forming the protein's distal heme pocket.

The atoms most immediately influenced by the photolysis event are those that undergo "through projectile" energy transfer. The dissociated ligand collides with heme pocket residues including surrounding isoleucine, leucine, and phenylalanine residues forming the heme pocket. Evident in Figure 4 is the early flash of "through projectile" heating of a cluster of heme pocket residues following collisions with the initially supersonic dissociated ligand. The collisional energy transfer and relaxation of the ligand occurs on a subpicosecond time scale as was noted in the simulation study of Straub and Karplus[7] in agreement with ultrafast experimental studies.[27,43,44]

At intermediate (short) times, excitation of residues flanking the heme occurs by a "through space" process of transfer from the out-of-plane vibrations of the excited heme. The process of diffusional energy transfer from the heme pocket residues excited by the ligand collisions continues. The first sign of "through bond" transfer of energy from the heme to the covalently bonded proximal histidine appears.

At longer times, the subsequent spreading of kinetic energy on the proximal side, outward from the excited proximal histidine residue, and the distal side, through pocket residues excited by the through projectile channel, continues. The result is a spatially anisotropic distribution of excess kinetic energy surrounding the heme.

Our observations argue against the validity of simple diffusional models that treat thermal diffusion through the protein matrix using a single, isotropic thermal diffusion constant. It may, however, be possible to construct a diffusion model based on a spatially dependent diffusion tensor derived from a knowledge of the protein's bond connectivity and values of the intrinsic friction derived from relaxation data such as that presented below and elsewhere.[24]

TABLE 2: Time Scales for the Convergence of the Kinetic Energy Metric in Solvated Myoglobin at 300 K[a]

region	$1/\gamma_0$ (ps)	time (ps)
total	0.47	1.25
protein	0.53	1.44
heme	0.15	0.72
solvent	0.13	0.75

[a] Total signifies the entire system consisting of myoglobin, the heme, and the solvent. The time scale is presented as (1) the reciprocal intrinsic friction, $1/\gamma 0$, and (2) the time for convergence of the kinetic energy metric to 1.0% of its original value.

3.4. Spatial Aniostropy in Kinetic Energy Relaxation. Attempts have been made to assign local atomic friction constants to atoms in proteins.[45,46] Some of those attempts have sought to describe the system using a single atomic frictional damping constant, a distribution of friction constants acting on zero temperature normal modes and dependent on the frequency of the particular mode,[47] or frictional constants dependent on the exposed surface area of a given protein atom.[48] Recently, it has been demonstrated that there is a strong spatial dependence on the rate of kinetic energy relaxation in myoglobin that is strongly dependent on the chemical character of the amino acid residue, and the nature of the group beit protein, heme chromophore, or solvent.[24] In this work, we have demonstrated that the most effective channel for rapid kinetic energy relaxation is through rapid equipartition within the heme followed by effective energy transfer to the solvent. Using a direct measure of the local atomic friction constants, we can interpret this observation in terms of the spatial dependence of the relaxation rates.

The inverse kinetic energy fluctuation metric $\Omega(0)/\Omega(t)$ was computed as a function of time for the total system, the protein, the heme, and the solvent. The simulations were run at 300 K. Each data set consists of an average over ten 30 ps trajectories. The effective intrinsic friction constants, γ_0, were derived using eq 4.[24] Data for the individual contributions of the protein, the heme, and the solvent are listed in Table 2. These data illustrate the relative degree of damping felt by the atoms within the indicated subsets of the solvated myoglobin system. The effective frictional forces acting on the atoms of the heme and the solvent molecules are considerably higher than those acting on the atoms of the protein. In fact, the average effective friction constant for the atoms of the heme is approximately *three times larger* than the effective friction acting on a typical atom of the protein itself. It should be kept in mind that the kinetic energy metrics discussed thus far describe energy redistribution within the moiety itself (heme, solvent, or protein) and do not necessarily indicate a transfer of energy from one moiety to another (heme $\rightleftharpoons$ protein, protein $\rightleftharpoons$ solvent, or solvent $\rightleftharpoons$ heme).

It is well appreciated that there is rapid intramolecular vibrational relaxation (IVR) within the heme. The heme group has a large and dense manifold of states, making it likely that energy will redistribute quickly. The heme group and its host protein share only one bond, that between the proximal histidine and the iron atom. The heme position is stabilized by roughly 90 van der Waals contacts. As such, the environment is not unlike that of a molecule in solution, the solute is the heme and the solvent is the protein and surrounding waters.

A threshold of the decay of the kinetic energy fluctuation metric $\Omega(t)$ to 1/100th of its initial value was used as an indication of sufficient convergence.[42] The time scales for ergodic convergence were assigned and the results are listed in Table 2. The rate at which the kinetic energy self-averages is remarkably rapid. Each component of the system reaches thermalization within a few picoseconds. Furthermore, the data show that the kinetic energy is rapidly redistributed within the heme and the solvent; energy transfer to the protein occurs more slowly. The time scales for this redistribution are similar for both the heme and solvent molecules, whereas the time scale for the protein is approximately a factor of 2 slower. These results suggest that the solvent could provide an important doorway for the flow of energy out of the heme.

4. Summary and Conclusions

Simulations of the process of ligand photolysis in solvated myoglobin indicate that the relaxation of kinetic energy occurs through a spatially aniostropic "funneling" mechanism first proposed by Hochstrasser and co-workers.[37] The dominant channel for relaxation of the excess kinetic energy in the heme moiety proceeds in two steps: rapid equipartitioning of kinetic energy within the heme followed by through space collisional energy transfer from the heme side chains to nearby solvating water molecules. Our simulations indicate that the heme's kinetic energy is found to relax according to an exponential process with a single time constant of roughly 5.9 ps.

Lim, Jackson, and Anfinrud observed the cooling of electronically relaxed heme in myoglobin following photoexcitation.[35] They observed a single-exponential decay with a time constant for heme cooling of 6.2 ± 0.5 ps. The observations derived from our simulations of heme cooling in solvated myoglobin are in close agreement with their result in both the single-exponential nature of the process and the exact value of the time constant.

The less effective channel of energy transfer from the heme to the protein is found to occur by three mechanisms: the initial and rapid "through projectile" energy transfer, due to collisions of the photolyzed ligand with nearby distal heme pocket residues, "through bond" energy transfer, which initially occurs solely through the bond of the heme iron to the proximal histidine, and the relatively less important "through space" nonbonded collisional energy transfer to nearby heme packing residues. The highly anisotropic diffusion of energy through the protein is determined by the details of the protein's architecture (of division by the heme into locally proximal and distal regions) and the mechanism of initiation of energy transfer (by photolysis of the ligand which is projected toward the distal heme pocket and relaxation of the heme geometry through bonding to the proximal histidine residue).

Our results support the conclusion that models of thermal diffusion through the protein must account for the factors of high spatial inhomogeneity in the local relaxation rates (of protein residues, heme, and solvent), bond connectivity, and the details of the initial heating (by ligand photolysis or direct excitation of the heme).

Acknowledgment. This work was supported in part by the Petroleum Research Fund of the American Chemical Society (34348-AC6), the National Science Foundation grant (CHE-9975494), and the National Institutes of Health through a NRSA F32-GM19273-01. We thank Lintao Bu and Francesca Massi for help in the preparation of the figures.

References and Notes

(1) Beece, D.; Eisenstein, L.; Frauenfelder, H.; Good, D.; Marden, M. C.; Reinisch, L.; Reynolds, A. H.; Sorensen, L. B.; Yue, K. T. *Biochem.* **1980**, *19*, 5147.

(2) Frauenfelder, H.; Wolynes, P. G. *Science* **1985**, *229*, 337.

(3) Steinbach, P. J.; Ansari, A.; Berendzen, J.; Braunstein, D.; Chu, K.; Cowen, B. R.; Ehrenstein, D.; Frauenfelder, H.; Johnson, J. B.; Lamb, D. C.; Luck, S.; Mourant, J. R.; Nienhaus, G. U.; Ormos, P.; Philipp, R.; Xie, A.; Young, R. D. *Biochemistry* **1991**, *30*, 3988. Mourant, J. R.; Braunstein, D. P; Chu, K.; Frauenfelder, H.; Nienhaus, G. U.; Ormos, P.; and Young, R. D. *Biophys. J.* 65: 1496, 1993; D. P. Braunstein, K. Chu, K. D. Egeberg, H. Frauenfelder, J. R. Mourant, G. U. Nienhaus, P. Ormos, S. G. Sligar, B. A. Springer and, R. D. Young. *Biophys. J.* 65: 2447, 1993.

(4) Elber, R.; Karplus, M. *Science* **1987**, *235*, 318.

(5) Elber, R.; Karplus, M. *J. Am. Chem. Soc.* **1990**, *112*, 9161.

(6) Kuczera, K. *Dynamics and Thermodynamics of Globins* In *Recent Developments in Theoretical Studies of Proteins*; World Scientific: Singapore, 1996.

(7) Straub, J. E.; Karplus, M. *Chem. Phys.* **1991**, *158*, 221.

(8) Meller, J.; Elber, R. *Biophys. J.* **1998**, *74*, 789.

(9) Sagnella, D. E.; Straub, J. E. *Biophys. J.* **1999**, *108*, 70.

(10) Li, H.; Elber, R.; Straub, J. E. *J. Biol. Chem.* **1993**, *24*, 17908.

(11) Ma, J.; Huo, S.; Straub, J. E. *J. Am. Chem. Soc.* **1997**, *119*, 2541.

(12) Vitkup, D.; Petsko, G.; Karplus, M. *Nat. Struct. Biol.* **1997**, *4*, 202.

(13) Genberg, L.; Heisel, F.; McLendon, G.; Miller, R. J. D. *J. Phys. Chem.* **1987**, *91*, 5521.

(14) Miller, R. J. D. *Acc. Chem. Res.* **1994**, *27*, 145.

(15) Genberg, L.; Richard, L.; McLendon, G.; Miller, R. J. D. *Science* **1991**, *251*, 1051.

(16) Mizutani, Y.; Kitagawa, T. *Science* **1997**, *278*, 443.

(17) Anfinrud, P. A.; Han, C.; Hochstrasser, R. M. *Proc. Natl. Acad. Sci. U.S.A.* **1989**, *86*, 8387.

(18) Nesbitt, D. J.; Hynes, J. T. *J. Chem. Phys.* **1982**, *77*, 2130.

(19) Rey, R.; Hynes, J. T. *J. Chem. Phys.* **1998**, *1*, 142.

(20) Gnanakaran, S.; Hochstrasser, R. M. *J. Phys. Chem.* **1996**, *100*, 3486.

(21) Egerov, S. A.; Skinner, J. L. *J. Chem. Phys.* **1996**, *105*, 7047.

(22) Everitt, K. F.; Egerov, S. A.; Skinner, J. L. *Chem. Phys.* **1998**, *235*, 115.

(23) Sagnella, D. E.; Lim, M.; Jackson, T.; Anfinrud, P. A.; Straub, J. E. *Proc. Natl. Acad. Sci. U.S.A.* **1999**, *96*, 14324.

(24) Sagnella, D. E.; Straub, J. E.; Thirumalai, D. *J. Chem. Phys.* **2000**, *113*, 7702.

(25) Greene, B. I.; Weissman, R. B.; Hochstrasser, R. M.; Eaton, W. A. *Proc. Natl. Acad. Sci. U.S.A.* **1978**, *75*, 5255.

(26) King, J. C.; Zhang, J. Z.; Schwartz, B. J.; Harris, C. B. *J. Chem. Phys.* **1993**, *99*, 7595.

(27) Anfinrud, P. A.; Han, C. H.; Lian, T. Q.; Hochstrasser, R. M. *J. Phys. Chem.* **1991**, *95*, 574.

(28) Nelson, A. G.; Nelson, K. A. *Chem. Phys.* **1991**, *152*, 69.

(29) Ansari, A.; Berendzen, J.; Bowne, S. F.; Frauenfelder, H.; Iben, I. E. T.; Sauke, T. B.; Shyamsunder, E.; Young, R. D. *Proc. Natl. Acad. Sci. U.S.A.* **1985**, *82*, 5000.

(30) Mizutani, Y.; Kitagawa, T. (The Chemical Record, in press).

(31) Henry, E. R.; Eaton, W. A.; Hochstrasser, R. M. *Proc. Natl. Acad. Sci. U.S.A.* **1986**, *83*, 8982.

(32) Petrich, J. W.; Poyart, C.; Martin, J. L. *Biochemistry* **1988**, *27*, 4049.

(33) Lingle, R.; Xu, X.; Zhu, H. P.; Yu, S. C.; Hopkins, J. B. *J. Phys. Chem.* **1991**, *95*, 9320.

(34) Li, P.; Sage, J. T.; Champion, P. M. *J. Chem. Phys.* **1992**, *97*, 3214.

(35) Lim, M. H.; Jackson, T. A.; Anfinrud, P. A. *J. Phys. Chem.* **1996**, *100*, 12 043.

(36) Miller, R. J. D. *Annu. Rev. Phys. Chem.* **1991**, *42*, 581.

(37) Lian, T.; Locke, B.; Kholodenko, Y.; Hochstrasser, R. M. *J. Phys. Chem.* **1994**, *98*, 11 648.

(38) Schlichting, I.; Berendzen, J.; Phillips, G. N.; Jr.; Sweet, R. M. *Nature* **1994**, *371*, 808.

(39) Jorgensen, W. L.; Chandrasekhar, J.; Madura, J. D.; Impey, R. W.; Klein, M. L. *J. Chem. Phys.* **1983**, *79*, 926.

(40) Mackerell, A. D., Jr.; Bashford, D.; Bellott, M.; Dunbrack, R. L., Jr.; Field, M. J.; Fischer, S.; Gao, J.; Guo, H.; Ha, S.; Joseph, D.; Kuchnir, L.; Kuczera, K.; Lau, F.; Mattos, C.; Michnick, S.; Ngo, T.; Nguyen, D. T.; Prodhom, B.; Roux, B.; Schlenkrich, M.; Smith, J. C.; Stote, R.; Straub, J.; Wiorkiewicz-Kuczera, J.; Karplus, M. *FASEB Journal* **1992**, *6*, A143.

(41) Brooks, B. R.; Bruccoleri, R. D.; Olafson, B. O.; States, D. J.; Swaminathan, S.; Karplus, M. *J. Comput. Chem* **1983**, *4*, 187.

(42) Thirumalai, D.; Mountain, R. D. *Phys. Rev. A* **1990**, *42*, 4574.

(43) Anfinrud, P. A.; Lim, M.; Jackson, T. A. *Proc. SPIE-Int. Soc. Opt. Eng.* **1994**, *2138*, 107.

(44) Anfinrud, P. A.; Lim, M.; Jackson, T. A. *Nat. Struct. Bio.* **1997**, *4*, 209.

(45) Kitao, A.; Hirata, F.; Gō, N. *Chem. Phys.* **1991**, *158*, 447.

(46) Hayward, S.; Kitao, A.; Hirata, F.; Gō, N. *J. Mol. Bio.* **1993**, *234*, 1207.

(47) Smith, J.; Cusack, S.; Tidor, B.; Karplus, M. *J. Chem. Phys.* **1990**, *93*, 2974.

(48) Ansari, A. *J. Chem. Phys.* **1999**, *110*, 1774.